THE JOURNAL OF BIOLOGICAL CHEMISTRY VOL. 281, NO. 11, pp. 7282–7293, March 17, 2006

Mitochondrial and Nuclear Forms of Wnt13 Are Generated via Alternative Promoters, Alternative RNA Splicing, and Alternative Translation Start Sites*

Received for publication, October 13, 2005, and in revised form, December 12, 2005 Published, JBC Papers in Press, January 6, 2006, DOI 10.1074/jbc.M511182200

Ian T. Struewing, Agata Toborek, and Catherine D. Mao[1]

From the Graduate Center for Nutritional Sciences, University of Kentucky, Lexington, Kentucky 40536

Wnt proteins play a key role in cell survival, cell proliferation, and cell fate during development. In endothelial cells, we identified the expression of Wnt13A, Wnt13B, and Wnt13C mRNAs, which are generated by alternative promoters and alternative RNA splicing. Wnt13A and Wnt13B proteins differ only in their N-terminal sequences. Wnt13A, a typical Wnt, is *N*-glycosylated and localized in the endoplasmic reticulum, with only a small fraction being secreted. Wnt13B proteins appear as a protein doublet, L-Wnt13B and S-Wnt13B, which are neither *N*-glycosylated nor secreted. Wnt13B proteins localized mainly to mitochondria, as demonstrated using detection in mitochondria enriched fractions and colocalization with Mitotracker and HSP60. A nuclear localization was also observed in 20% of Wnt13B-expressing cells. Both the N-terminal hydrophobic stretch (residues 1–17) and α-helix (residues 26–50) were the main determinants for Wnt13B mitochondrial targeting. Serial deletions of Wnt13B N-terminal sequences abolished its association with mitochondria and favored instead a nuclear localization. The production of S-Wnt13B was independent of the mitochondrial targeting but dependent on an alternative translation start corresponding to Met^{74} in L-Wnt13B. The same translation start is used in Wnt13C mRNA to encode a protein undistinguishable from S-Wnt13B. S-Wnt13B when expressed alone localized to the nucleus like Wnt13C, whereas L-Wnt13B localized to mitochondria. Wnt13 nuclear forms increased the β-catenin/T-cell factor activity in HEK293 cells and increased apoptosis in bovine aortic endothelial cells. Altogether our results demonstrate that, in addition to alternative promoters and RNA splicing, an alternative translation start in Wnt13B and Wnt13C mRNAs increases the complexity of both human *wnt13* expression and functions.

Wnt proteins are cysteine-rich glycoproteins that play diverse functions during development, including control of cell fate and cell proliferation, establishment of cell polarity, and initiation of cell migration (1). Wnt proteins elicit most of these activities through binding with the seven-transmembrane Frizzled receptors (2) and with the co-receptors low density lipoprotein receptor-related protein-5 and -6 (3). Depending upon the combination of Wnt ligands and Frizzled receptors, three different signaling pathways have been identified. All three pathways involve common downstream protein adaptors, the disheveled/Dvl proteins (4, 5). The canonical Wnt/β-catenin pathway leads to the stabilization of cytoplasmic β-catenin, which subsequently translocates to the nucleus, where it binds to the transcription factors of the T-cell factor (TCF)[2] family and regulates the expression of genes involved in cell cycle and cell adhesion (6). The Wnt/Ca^{2+}-dependent pathway is a classical G-protein-coupled receptor pathway leading to the activation of protein kinase C and Ca^{2+}-calmodulin-dependent kinase II (7). The Wnt/planar cell polarity pathway leads to the activation of the small GTPases of the Rho family, Rho A, Rac 1, and Cdc42, which in turn regulate the cytoskeleton and thus cell morphology and migratory behaviors (8, 9).

In mammals, 19 different Wnt family members displaying a conserved pattern of 21–23 cysteine residues have been identified so far. Although a high similarity exists between them, their roles *in vivo*, as identified by specific knock-out in mice, are not redundant (1, 10). *wnt* genes are often expressed in a spatial and temporal fashion, which accounts for the major part of their specific activity. In addition, Wnt proteins also display divergent N-terminal sequences that account for their differential ability to be secreted (11). Although Wnt proteins are found secreted and associated with the extracellular matrix (ECM), the efficiency of secretion is very poor, and most of the Wnt proteins are mainly retained in the endoplasmic reticulum (ER) despite the lack of ER retrieval and ER retention consensus sequences (12). Retention in the ER is dependent upon the interaction of the Wnt proteins with the ER chaperone Grp78/BiP (11, 13). Efficient secretion of the Wnt proteins, both in *Drosophila* and mammalian cells, requires the expression of Porcupine, a transmembrane protein located in the ER with a putative acyltransferase activity (14–16). Porcupine binds a conserved region in the N terminus of the Wnt proteins surrounding the *N*-glycosylation site and favors their *N*-glycosylation by a mechanism that remains yet to be identified (17). Recently, Wnt3A, Wnt8, and Dwnt1 proteins were found to be lipid-modified, in particular by the addition of palmitate on a conserved cysteine (Cys^{77} in Wnt3A) present in the interaction domain with Porcupine (18, 19), hence reinforcing the concept of an association of the Wnt proteins with membrane compartments, such as the ER and secretory vesicles. Altogether these results emphasize the importance of determining the cellular processing and targeting of the Wnt proteins in order to understand their mechanism of action and/or the regulation of their activity.

The *wnt13* gene, also called *wnt2b*, is one of the rare *wnt* genes that gives rise to different mRNA forms by alternative splicing (20). In adult gastric epithelial cells, two Wnt13/Wnt2B mRNA forms were found expressed, Wnt13A/Wnt2B2 and Wnt13B/Wnt2B1, which code for

* This work was supported by National Institutes of Health Grant HL68698 (to C. D. M.). The costs of publication of this article were defrayed in part by the payment of page charges. This article must therefore be hereby marked "*advertisement*" in accordance with 18 U.S.C. Section 1734 solely to indicate this fact.

[1] To whom correspondence should be addressed: Graduate Center for Nutritional Sciences, University of Kentucky, 900 Limestone St., Lexington, KY 40536. Tel.: 859-323-4933 (ext. 81377); Fax: 859-257-3646; E-mail: cdmao2@uky.edu.

[2] The abbreviations used are: TCF, T-cell factor; BAEC, bovine aortic endothelial cell(s); HUVEC, human umbilical vein endothelial cell; HEK293 cells, human embryonic kidney 293 cells; ER, endoplasmic reticulum; HSP, heat shock protein; PBS, phosphate-buffered saline; CM, conditioned media; ECM, extracellular matrix; TNF, tumor necrosis factor; CHAPS, 3-[(3-cholamidopropyl)dimethylammonio]-1-propanesulfonic acid; aa, amino acid(s).

TABLE 1
Sequence of the PCR primers used in this study

Constructs	Primer sequences
Full-length	
Wnt13A	fwd: 5′-CATGCTGAGACCGGGTGG-3′; rev: 5′-GTTCAGGTCTGGTCCAGCC-3′
Wnt13B/Wnt13C	fwd: 5′-CATGTTGGATGGCCTTGGAG-3′; rev: 5′-GTTCAGGTCTGGTCCAGCC-3′
Wnt13-FLAG tag	rev: 5′-TCACTTATCGTCGTCATCCTTGTAATCTGCGGTCTGGTCCAGCCAC-3′
Expression	
Wnt13A	fwd: 5′-CGTAGACACGTCCTGGTGGTA-3′; rev: 5′-GCTGACACTCTCGGATCCAT-3′
Wnt13B/Wnt13C	fwd: 5′-CATGTTGGATGGCCTTGGAG-3′; rev: 5′-GCTGACACTCTCGGATCCAT-3′
Chimera	
Wnt13AB	fwd: 5′-CATGCTGAGACCGGGTGG-3′; rev: 5′-GCAGAAGGCATGCAAGACCTAGG-3′; fwd: 5′-CCTTGAGGACGGCATGCCCTGGCATACC-3′; rev: Wnt13-FLAG tag primer
Wnt13BA	fwd: 5′-CATGTTGGATGGCCTTGGAG-3′; rev: 5′-GGTATGCCAGGGCATGCCGTCCTCAAGG-3′ fwd: 5′-CCTAGGTCTTGCATGCCTTCTGC-3′; rev: Wnt13-FLAG tag primer
Deletions	
Δ(1–17)Wnt13B	fwd: 5′-GCCACCATGAAAACTGAAGGATCCTTG-3′, rev: Wnt13-FLAG tag primer
Δ(1–52)Wnt13B	fwd: 5′-GCCACCATGGGGGCACGAGTGATCTG-3′; rev: Wnt13-FLAG tag primer
Δ(1–88)Wnt13B	fwd: 5′-CCACCATGCAGCACCAATTCCGCCAC-3′; rev: Wnt13-FLAG tag primer
Targeted mutations	
C88A-Wnt13	S: 5′-CCCGAGAATGGATCCGAGAGGCTCAGCACCAATTCCGCCACCACC-3′
R50A-Wnt13B	S: 5′-GGGCACTGGGGGCAGCAGTGATCTGTGACAATATCC-3′
K38,R42-Wnt13B	S: 5′-CCTACACAGTCAGCGTTCAACGCGTGTTTGCAAGCGTACATTGGGGCACTGGGGC-3′
R69G-Wnt13	S: 5′-GCCGGCAGCGGCAGCTGTGCCAGGGTTACCCAGACATCATGCGTTCAG-3′
R62A,R64A-Wnt13	S: 5′-CCCTGGTTTGGTGAGCGCGCAGGCGCAGCTGTGCCAGGGTTACC-3′
M74L-Wnt13	S: 5′-CGTTACCCAGACATCTTGCGTTCAGTGGGC-3′
M1L-Wnt13B	S: 5′-GCCACCCTGTTGGATGGCCTT-3′
D72E-Wnt13	S: 5′-CCAGCGTTACCCAGAAATCATGCGTTCAGTGG-3′
R75A-Wnt13	S: 5′-CGTTACCCAGACATCATGGCTTCAGTGGGCGAGGG-3′

proteins that differ only by their N-terminal sequences (20). During chick development of the retina, *wnt13* was expressed in particular at the marginal tip of the retina, where it maintains undifferentiated progenitor cells in the ciliary marginal zone (21, 22). These effects of Wnt13 were associated with the activation of the canonical β-catenin/LEF/TCF signaling pathway (23). Another role as a morphogen was also described in the chick retina, where *wnt13* expression in the anterior rim allows the proper development of laminated retinal layers (24). Although the particular form of Wnt13 expressed in this study was not defined, it probably refers to Wnt13A/Wnt2B2, since only Wnt13A/Wnt2B2 proteins, and not Wnt13B/Wnt2B1, were able to activate the canonical β-catenin/TCF pathway and induce axis duplication in *Xenopus* embryo (25).

We have identified the expression of three different mRNA forms of the *wnt13* gene in endothelial cells of different origins: the previously described Wnt13A/Wnt2B2 and Wnt13B/Wnt2B1 mRNA forms (20) and an additional Wnt13C mRNA generated by an alternative splicing that skips exon 2 (Fig. 1). In this report, we demonstrate that these various Wnt13 mRNA isoforms code for proteins with distinct N termini, processing, and subcellular localizations. Whereas Wnt13A is a classical Wnt protein, *N*-glycosylated and secreted, Wnt13B and Wnt13C are intracellular forms targeted to mitochondria and to the nucleus respectively. Such different subcellular localizations for Wnt13A and Wnt13B proteins explain the differential activities previously observed for these two forms (25). In addition, these results strengthen the importance of the processing of Wnt proteins in relationship with their targeting and intracellular activities.

MATERIALS AND METHODS

Antibodies and Reagents—The polyclonal anti-FLAG antibodies were purchased from Cayman Chemical, and the M2-anti-FLAG-agarose gel was from Sigma. The monoclonal anti-HSP60, anti-KDEL peptide sequence, anti-AIF antibodies, and anti-Cu/Zn-superoxide dismutase (SOD1) antibodies were purchased from Stressgen, and the monoclonal anti-α-tubulin antibodies were from Sigma. The cleaved caspase-3, caspase-3, and cAMP-responsive element-binding protein antibodies were purchased from Cell Signaling. The monoclonal anti-cytochrome *c* antibodies, clone 7H8.2C12, were from BD PharMingen and the goat polyclonal anti-calnexin was from Santa Cruz Biotechnology, Inc. The secondary goat anti-rabbit and goat anti-mouse antibodies conjugated to horseradish peroxidase were from Cell Signaling, whereas the donkey anti-goat antibodies, horseradish peroxidase-conjugated, were from Jackson Laboratories. Mitotracker-Deep Red-633 and the secondary goat anti-rabbit and goat anti-mouse antibodies conjugated either with Alexa-488 or Alexa-568 were from Molecular Probes, Inc. The inhibitors tunicamycin, MG132, and ALLN, were obtained from Sigma, and the inhibitors benzyloxycarbonyl-VAD-fluoromethyl ketone and the permeable metalloprotease inhibitor type III were purchased from Calbiochem. Recombinant tumor necrosis factor (TNF)-α was from R&D Systems.

Wnt13-FLAG Constructs—Full-length Wnt13A, Wnt13B, and Wnt13C cDNAs were obtained using total RNAs extracted from BAEC and HUVEC respectively and reverse transcription-PCR with the primers described in Table 1. After elimination of the stop codon, the FLAG sequence (DYKDDDDK) was added in frame with the first ATG at the C terminus of each Wnt13 cDNAs, and the resulting cDNAs were cloned into pCR3.1 vector (Invitrogen). All of the N-terminal deletion mutants, Δ(1–17)Wnt13B, Δ(1–52)Wnt13B, and Δ(1–88)Wnt13B, were obtained by PCR using the upstream primers as indicated in Table 1 and the FLAG tag reverse primer. All the mutations resulting in single and multiple aa changes in the Wnt13B-FLAG construct were obtained by PCR using the QuikChange kit (Stratagene) with the various primers described in Table 1 and with either Wnt13B-FLAG or the appropriate mutated Wnt13B-FLAG constructs as template. The chimeric N-terminal constructs Wnt13AB (Wnt13A-(1–42) + Wnt13B-(26–372)) and Wnt13BA (Wnt13B-(1–25) + Wnt13A-(43–391)) were generated after insertion of a SphI site by PCR in both Wnt13A-FLAG and Wnt13B-FLAG cDNA sequences, respectively, at positions +126 and +79 using PCR. The swapping of the N-terminal sequences was obtained after SphI restriction digest and ligation with the C-terminal sequences of either Wnt13A or Wnt13B. The integrity of each construct was verified by sequencing. The YC4-mit plasmid coding for the mito-

chondria matrix-targeted green fluorescent protein was used as control in the transfection experiments (26).

Cell Culture and Transfection—The endothelial primary cells, HUVEC and BAEC, were isolated as previously described (27) and maintained in MCDB105 (Sigma) supplemented with 20% fetal bovine serum and in Dulbecco's modified Eagle's medium plus 4.5 g/liter glucose (Invitrogen) supplemented with 10% fetal bovine serum (BioWhittaker), respectively. The human microvascular endothelial cell line HMEC-1 and the epithelial cell line HEK293 were maintained also in Dulbecco's modified Eagle's medium plus 4.5 g/liter glucose, supplemented with 10% fetal bovine serum. Transient transfections of BAEC and HEK293 cells with the various constructs were performed using Exgen 500 reagent (MBI Fermentas) as recommended by the manufacturer.

Analysis of Wnt13 mRNA Expression—Total RNAs (1 μg) were subjected to DNase I treatment for 15 min at 20 °C to remove any DNA contaminations prior to the addition of 0.5 μg of oligo(dT)$_{12-18}$ primers and 10 units of the SuperScript reverse transcriptase for 50 min at 42 °C according to the manufacturer (Invitrogen). cDNAs for Wnt13A and for Wnt13B/C were amplified by 40 cycles of PCR using forward primers specific for exon 3 (5′-CGTAGACACGTCCTGGTGGTA-3′) and exon 1 (5′-CATGTTGGATGGCCTTGGAG-3′), respectively, and a universal Wnt13 reverse primer located in exon 4 (5′-GCTGACACTCTCGGATCCAT-3′). The expression of the ribosomal protein L32 mRNA was used as internal control, and rpL32 cDNAs were amplified for 25 cycles of PCR with rpL32-fwd primer (5′-GCCAGATCTTGATGCCCAAC-3′) and rpL32-rev primer (5′-CGTGCACATGAGCTGCCTAC-3′).

Cell Extracts, Immunoprecipitation, and Western Blot Analysis—For whole cell extracts, the cells were harvested and lysed in 50 mM Tris-HCl buffer, pH 7.5, containing 150 mM NaCl, 1% Triton X-100, 1 mM EDTA in the presence of protease and phosphatase inhibitor mixtures (Sigma). Insoluble fraction pellets were discarded after centrifugation at 20,000 × *g* for 20 min at 4 °C. For cell fractionation, the conditioned media (CM) were collected, and the cells were washed with cold PBS prior to being detached from the plates with cold PBS containing 5 mM EDTA and 5 mM EGTA. The detached cells were collected and processed as described below; meanwhile, the plates were washed extensively with ice-cold water to eliminate residual cells, and the ECM components were dissociated from the plates with denaturing Laemmli buffer. The cells were centrifuged at 400 × *g* for 5 min at 4 °C. Cell pellets were suspended in hypotonic buffer (50 mM HEPES, pH 7.5, 1.5 mM $MgCl_2$, 1 mM EDTA supplemented with protease and phosphatase inhibitor mixtures) and incubated on ice for 30 min prior to being subjected to 20 passages through 26-gauge needles to disrupt the cells. The nuclei and cytoskeleton fractions were obtained by centrifugation at 1,200 × *g* for 5 min at 4 °C (pellet), and the resulting supernatants were further subjected to 100,000 × *g* for 30 min at 4 °C to obtain the membrane fractions (pellet) and the cytosolic fractions (supernatant). The nuclei and membrane pellets were suspended and dissolved in the hypotonic buffer supplemented with 1% Triton X-100 and 150 mM NaCl, and the insoluble fractions were discarded after centrifugation at 20,000 × *g* for 20 min. The cytosolic fractions were adjusted to 150 mM NaCl and 1% Triton X-100 final concentration, and the CM were supplemented with a protease inhibitor mixture and adjusted to 1% Triton X-100. For immunoprecipitation of the FLAG-tagged proteins, the various cell fractions or whole lysates were incubated with 20 μl of M2-anti-FLAG-agarose beads for 16 h at 4 °C. After extensive washes, proteins bound to the beads were eluted with 20 μl of denaturing Laemmli buffer. For Western blot analysis, proteins were fractionated on polyacrylamide-SDS gels and transferred onto Immobilon P membrane (Millipore Corp.). After blocking, the membranes were incubated with the various primary antibodies as indicated and subsequently with the appropriate secondary antibodies conjugated to horseradish peroxidase (Cell Signaling). Immunoreactive proteins were detected using SuperSignal® chemiluminescence (Pierce).

Mitochondria Isolation and Biochemical Analysis—Mitochondria were prepared as previously described (28). Briefly, BAEC were harvested 24 h post-transfection and suspended in 500 μl of homogenizing buffer (250 mM sucrose, 20 mM Hepes, pH 7.5, 10 mM KCl, 1.5 mM $MgCl_2$, supplemented with protease and phosphatase mixture inhibitors). After incubation on ice for 30 min, the cells were disrupted by 20 passages through 26-gauge needles. Unbroken cells and nuclei were removed by centrifugation at 400 × *g* for 5 min at 4 °C. The resulting supernatant was centrifuged at 8,000 × *g* for 15 min to obtain the mitochondria enriched pellets. After an additional wash in the homogenizing buffer, the crude mitochondria preparation was used either for immunoprecipitation or biochemical analyses. For BAEC subcellular fractionations, this protocol was modified as follows. The cell disruption step was repeated twice, and the various subcellular fractions were obtained by differential centrifugations: nuclear pellet, 400 × *g* for 5 min; mitochondria pellet, 8,000 × *g* for 10 min; ER pellet, 25,000 × *g* for 10 min; and cytosol plus light membrane fraction, 25,000 × *g* supernatant. Each obtained pellet was washed twice in the homogenizing buffer prior to analysis. The association of Wnt13B with mitochondria was tested using high salt and alkaline extraction as previously described (29). Briefly, mitochondria were suspended in the homogenizing buffer in the absence or presence of either 1 M KCl or 100 mM sodium carbonate, pH 11, and incubated on ice for 30 min prior to centrifugation at 10,000 × *g* for 15 min for obtaining the mitochondria pellet and the supernatant containing extracted mitochondrial proteins. The supernatants and mitochondria pellets were analyzed by Western blotting. For the immunoprecipitation experiments, mitochondria were homogenized in 50 mM HEPES, pH 7.5, 150 mM NaCl, 1.5 mM $MgCl_2$, 1% Triton supplemented with protease and phosphatase mixture inhibitors, and the FLAG-tagged proteins were purified by chromatography using the M2 anti-FLAG-agarose beads as described above. The immunoprecipitated proteins were analyzed by Western blotting.

Immunofluorescence and Confocal Microscopy—BAEC were plated in LabTek slide chambers coated with fibronectin (1 μg/cm^2) (Invitrogen) 24 h prior to transfection. 24 h post-transfection, when required, mitochondria were stained with Mitotracker-633 deep red for 45 min as recommended by the manufacturer prior to cell washes with PBS supplemented with 1 mM $CaCl_2$ and 1 mM $MgCl_2$ and fixation in 4% formaldehyde. Cells were permeabilized and blocked in PBS, 0.1% Triton X-100, 0.7% fish skin gelatin (Sigma) at 37 °C for 30 min followed by sequential incubations with primary antibodies and Alexa-secondary antibodies for 2 h each in the same buffer. Nuclei were stained with 4′,6-diamidino-2-phenylindole during slide mounting with Vectashield H1200 (Vector Laboratories Inc.). Images were taken with a Leica confocal upright microscope every 1 μm throughout the heights of the cells at either × 64 or × 100 magnification, and maximum average images were recorded. At least four independent transfections and staining experiments were done, and representative images are shown.

Luciferase Assays—HEK293 cells were plated in 12-well culture clusters and 24 h later transiently cotransfected with 5 ng of phRG-TK plasmid as control for the efficiency of transfection (Promega), 250 ng of the TOP-Flash or FOP-Flash luciferase constructs containing, respectively, wild-type or mutated TCF binding sites upstream of the minimal thymidine kinase promoter (30), 300 ng of pcDNA3-S37A-β-catenin

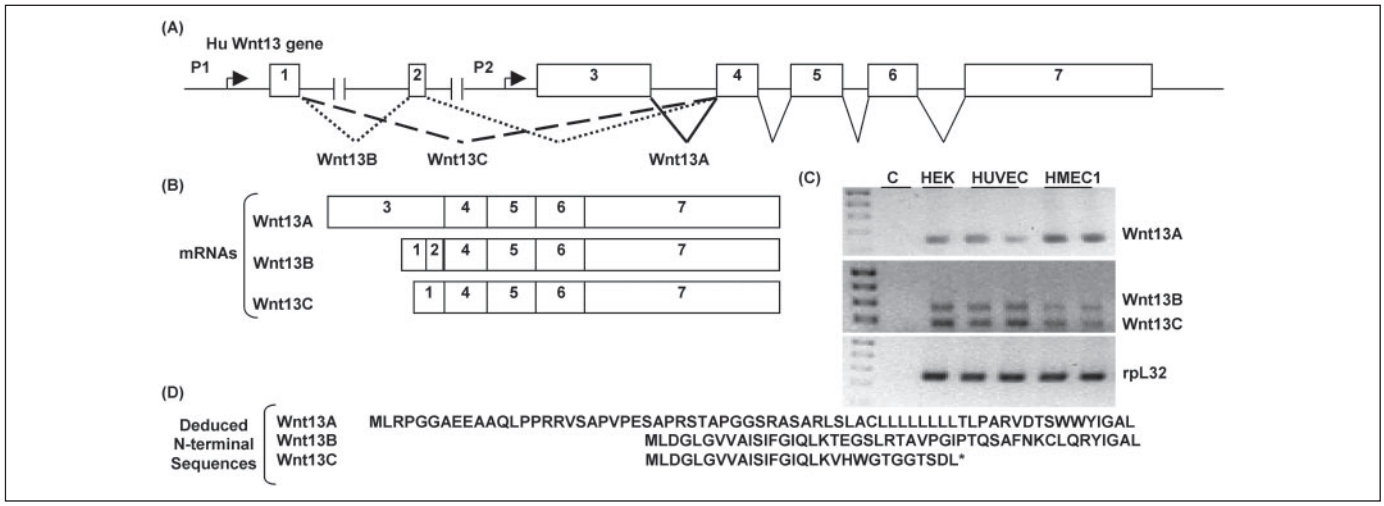

FIGURE 1. **Expression of three Wnt13 mRNA isoforms in differentiated endothelial cells.** Shown is a schematic representation of the organization of the human *wnt13* gene (*A*) and the different mRNA isoforms expressed in human endothelial cells (*B*). *C*, analysis of the expression of Wnt13A, Wnt13B, and Wnt13C mRNA species by reverse transcription-PCR in HEK293 cells, in the primary endothelial cells HUVEC, and in the transformed endothelial cells HMEC1. *D*, the deduced N-terminal aa sequences for Wnt13A, Wnt13B, and Wnt13C starting from the first translation initiation codon encountered in the mRNAs are indicated.

plasmid, and 450 ng of the various Wnt13 expression constructs, as indicated. 24 h after transfection, the cells were lysed, and the *Renilla* and firefly luciferase assays were performed using the dual luciferase assay kit (Promega) and quantified using LmaxII luminometer (Molecular Devices). Five independent transfection experiments were performed in duplicates.

Analysis of the Induction of IL-8 mRNA Expression in HEK293 Cells by Real Time PCR—HEK293 cells (5×10^5 cells) were plated in 60-mm dishes and transfected 24 h later either with 4 μg of PCR3 vector as control, 2 μg of S37A-β-catenin + 2 μg of PCR3 vectors, 2 μg of pCR3-M1L-Wnt13B + 2 μg of PCR3 vectors, or 2 μg of S37A-β-catenin + 2 μg of pCR3-M1L-Wnt13B vectors. Cells were harvested 24 h after transfection, and total RNAs were extracted with Trizol reagent (Invitrogen). Total RNAs (1 μg) were subjected to DNase I treatment and reverse transcription as previously described for the analysis of Wnt13 mRNA expression. Real time PCRs were conducted using the SyBr Green PCR kit and the ABI Prism 7000 sequence detector from PerkinElmer Life Sciences, and the relative levels of IL-8 cDNAs were determined using the threshold cycles (Ct value). The expression of rpL32 cDNA was used as an internal control, and the Ct values obtained for IL-8 were corrected for any variations of the Ct values of rpL32. The primers used for human IL-8 were as follows: forward, 5′-GTGCAGTTTTGCCAAGGAGTG-3′; reverse, 5′-CTCTGCACCCAGTTTTCCTTG-3′.

Analysis of Apoptosis in BAEC—BAEC were transiently transfected either with YC4-mit control plasmid, Wnt13A-FLAG, or the various Wnt13B-FLAG constructs for 24 h. The appearance of apoptotic nuclei in BAEC expressing the various proteins of interest was quantified using immunofluorescence microscopy after staining of both the nuclei with 4′,6-diamidino-2-phenylindole and the FLAG-tagged proteins with the polyclonal anti-FLAG antibodies. Activation of caspase-3 was determined by following the appearance of the active cleaved form of caspase-3 using Western blotting and the specific cleaved caspase-3 antibodies (Cell Signaling). For these experiments, BAEC expressing the various target proteins were treated with 5 ng/ml TNF-α for 12 h, prior to being lysed directly in denaturing Laemmli buffer. At least three independent experiments were performed for each of the apoptosis assays.

RESULTS

Endothelial Cells Express Three Different Wnt13 RNA Isoforms—Using the Wnt degenerate primers previously described (31) and cDNAs obtained from HUVEC and HMEC-1, we found that *wnt13* and *wnt5A* were the main *wnt* genes expressed in these differentiated endothelial cells (not shown). The cloning of full-length Wnt13 cDNAs from these cell lines gave three different cDNAs. Two cDNAs corresponded to the previously described Wnt13A/Wnt2b2 mRNA transcribed from the P2 promoter and composed of exons 3–7 and Wnt13B/Wnt2b1 mRNA transcribed from the P1 promoter and composed of exons 1 and 2 and exons 4–7 (Fig. 1, *A–C*). An additional Wnt13 cDNA corresponded to a novel Wnt13 mRNA species that was named Wnt13C. Wnt13C mRNAs are transcribed from the P1 promoter like Wnt13B mRNAs but are composed of exons 1 and 4–7, since the entire exon 2 is skipped during an alternative splicing (Fig. 1, *A–C*). The expression of these three Wnt13 mRNA species was also observed in the epithelial HEK293 cells (Fig. 1*C*). Wnt13B and Wnt13C mRNAs differ thus by the deletion of 71 nucleotides corresponding to exon 2 (Fig. 1*C*), and this deletion in Wnt13C leads to a change in the open reading frame of exon 4 and generation of a stop codon within exon 4. Consequently, the deduced amino acid sequence coded by Wnt13C mRNA from the first translation initiation codon in exon 1 is a very short peptide of 30 amino acids in length, whereas Wnt13A and Wnt13B mRNAs code for proteins that differ only by their N-terminal sequences (Fig. 1*D*).

Wnt13A and Wnt13B Display Different Processing and Subcellular Localizations—First, the role of these differential N-terminal sequences in the processing and cellular targeting of Wnt13A and Wnt13B proteins was assessed. Wnt13A-FLAG and Wnt13B-FLAG proteins were transiently expressed in BAEC for 24 h prior to collection of CM, recovery of the ECM, and cell fractionation. FLAG-tagged proteins were immunoprecipitated and analyzed by immunoblotting. Wnt13A-FLAG proteins were secreted as shown by their presence in the CM, although they were mainly retained in the membrane fraction (Fig. 2*A*). In contrast, Wnt13B-FLAG proteins were not secreted but were associated with the nuclei/cytoskeleton pellets and membrane fractions (Fig. 2*A*). Furthermore, Wnt13A-FLAG proteins migrated mainly as a single protein band with an apparent molecular mass of 42 kDa, whereas Wnt13B-FLAG proteins migrated as a doublet of proteins with apparent molec-

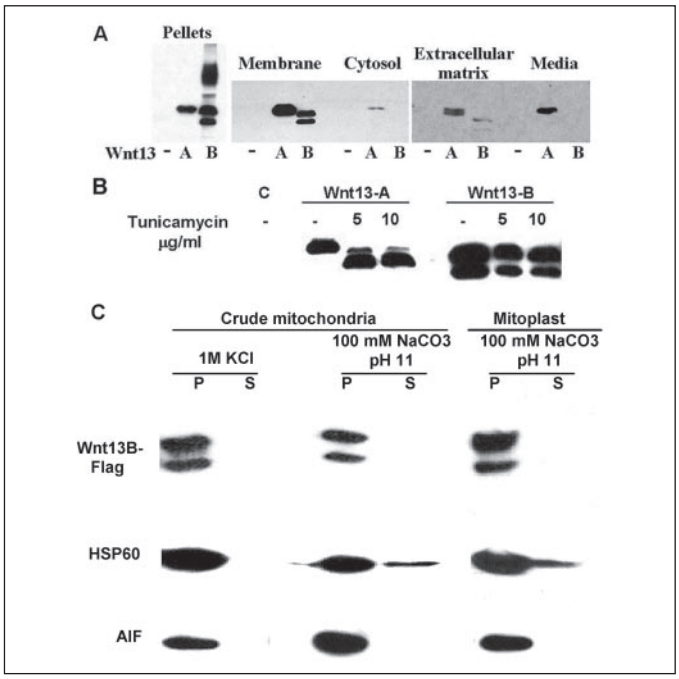

FIGURE 2. **Wnt13A-FLAG and Wnt13B-FLAG proteins display different subcellular localizations and post-translational modifications.** *A*, Western blot analysis of Wnt13A-FLAG and Wnt13B-FLAG localization by cell fractionation. BAEC were transfected with either control (−), Wnt13A-FLAG (*A*), or Wnt13B-FLAG (*B*) constructs, and 24 h later the CM were collected, the ECM components were isolated, and cell fractionations were prepared as described under "Materials and Methods." FLAG-tagged proteins were purified from the various cell fractions using M2-anti-FLAG-agarose affinity chromatography with the exception of the ECM fractions, where the total ECM extracts were directly analyzed. FLAG-tagged proteins were detected by immunoblotting. *B*, analysis of *N*-glycosylation modifications of Wnt13A-FLAG and Wnt13B-FLAG proteins. BAEC were transfected either with control (*C*), Wnt13A-FLAG, or Wnt13B-FLAG constructs, and 12 h later, the cells were treated either with vehicle (−) or with the indicated doses of the *N*-glycosylation inhibitor tunicamycin for a further 12-h incubation period. Whole cell extracts were prepared, and FLAG-tagged proteins were analyzed by immunoblotting. *C*, BAEC were transfected with the Wnt13B-FLAG construct for 24 h prior to preparing crude mitochondria fractions and mitoplast fractions. The enriched mitochondria and mitoplast fractions were subjected to either 1 M KCl or 100 mM carbonate buffer, pH 11, for 30 min on ice, as indicated, and after centrifugation at 8,000 × *g*, the mitochondrial membrane pellets (*P*) and the supernatants (*S*) were analyzed by immunoblotting for the presence of FLAG-tagged HSP60 and AIF proteins.

ular masses of 40 and 35 kDa, which will be referred to hereafter as long (L-Wnt13B) and short (S-Wnt13B) forms, respectively. Stable dimers of both Wnt13A-FLAG and Wnt13B-FLAG proteins were observed occasionally, although Wnt13B-FLAG proteins appeared to have a higher propensity to remain as stable dimers and higher size aggregates even after denaturation (see Fig. 2*A*, *Pellets*). Similar results were observed in other endothelial cells (HUVEC and HMEC1) as well as in HEK293 cells, although in the latter, the S-Wnt13B form was always the major form (not shown).

Wnt proteins are usually *N*-glycosylated, and this post-translational modification is required for Wnt protein secretion (17). To determine whether the Wnt13B-FLAG protein doublet resulted from different *N*-glycosylation events, BAEC were transiently transfected with either Wnt13B-FLAG construct or Wnt13A-FLAG construct as control and subjected to treatment with various doses of tunicamycin. As expected, the post-translational processing of Wnt13A-FLAG proteins was sensitive to tunicamycin treatment, and the appearance of a reduced size protein of 37 kDa corresponding to the unglycosylated form of Wnt13A was observed (Fig. 2*B*). In contrast, both L-Wnt13B and S-Wnt13B proteins were not affected by the tunicamycin treatment, revealing that none of Wnt13B forms are *N*-glycosylated in BAEC (Fig. 2*B*). Similar results were observed in HEK293 cells (not shown).

In addition to differential post-translational processing, Wnt13A and Wnt13B proteins displayed different subcellular localizations, as determined by immunofluorescence staining and confocal microscopy analysis. In BAEC, Wnt13A-FLAG proteins were associated with a thin reticular meshwork colocalizing with antibodies recognizing the KDEL peptide sequence present in proteins that are retained in the ER lumen (Fig. 3*A*). Therefore, like most of the Wnt protein members, Wnt13A-FLAG proteins were mainly retained in the ER, although they are lacking ER retention and retrieval sequences (12). In contrast, Wnt13B-FLAG proteins appeared in punctated structures associated with the microtubule network (Fig. 3*A*) but not with the ER marker (not shown). In both cases, there was no significant difference in β-catenin staining in BAEC expressing Wnt13A or Wnt13B proteins compared with nonexpressing cells; β-catenin was mainly associated with cell-cell contacts, and no translocation of endogenous β-catenin to the nucleus was observed (Fig. 3*A*). Similar localizations were obtained for both Wnt13A and Wnt13B proteins in HEK293 cells (not shown).

Wnt13B Localizes to Mitochondria and Induces Changes in Mitochondria Morphology—To further analyze the subcellular localization of Wnt13B-FLAG proteins, various markers of cellular organelles were tested, including markers of lysosome (LysoTracker and LAMP1) and markers of mitochondria (Mitotracker and HSP60). There was no clear and consistent co-localization of Wnt13B-FLAG proteins with both lysosome markers (not shown). In contrast, co-localization of Wnt13B-FLAG proteins with the mitochondrial marker Mitotracker was observed when the mitochondria morphology was reticular (Fig. 3*B*). However, in most cases, the expression of Wnt13B-FLAG proteins was associated with an alteration of mitochondria morphology, from a reticular to a fragmented morphology, and with a decreased accumulation of the Mitotracker dye in mitochondria (Fig. 3*B*). Nonetheless, the localization of Wnt13B-FLAG proteins to mitochondria was further confirmed by using the chaperone HSP60 as an additional mitochondrial marker (Fig. 3*C*). Wnt13B-FLAG proteins were clearly associated with HSP60 proteins even in the absence of mitotracker staining of mitochondria. In addition to this mitochondrial localization, around 10–20% of BAEC overexpressing Wnt13B-FLAG proteins also displayed nuclear staining (Fig. 3*C*). In contrast, Wnt13A-FLAG proteins were not found in nuclei and had no effect either on mitochondria morphology or on the accumulation of Mitotracker in mitochondria (Fig. 3*C*).

To confirm the mitochondrial localization of Wnt13B, crude mitochondria fractions were prepared from BAEC expressing Wnt13B-FLAG proteins. As shown in Fig. 2*C*, both L-Wnt13B and S-Wnt13B forms were present in the enriched mitochondrial fractions and remained associated with the mitochondrial pellets even in the presence of high salt concentration (1 M KCl), indicating that Wnt13B proteins are not peripherally associated with mitochondria. In addition, Wnt13B proteins remained associated with the membrane fractions of both mitochondria and mitoplasts after alkaline extraction (100 mM carbonate buffer, pH 11), indicating that Wnt13B proteins are tightly associated with mitochondrial membranes and, in particular, with the inner membranes (Fig. 2*C*). Wnt13B proteins behaved similarly to the apoptosis-inducing factor, an inner membrane-associated protein (47). In contrast, HSP60, a mitochondrial matrix protein, was significantly extracted by the alkaline treatment and found in the supernatant as expected (Fig. 2*C*). The tight association of Wnt13B with membranes is further supported by its requirement for solubility/extraction of strong detergents such as CHAPS or SDS, whereas only 50% of solubility is achieved with 1% Triton X-100 (not shown).

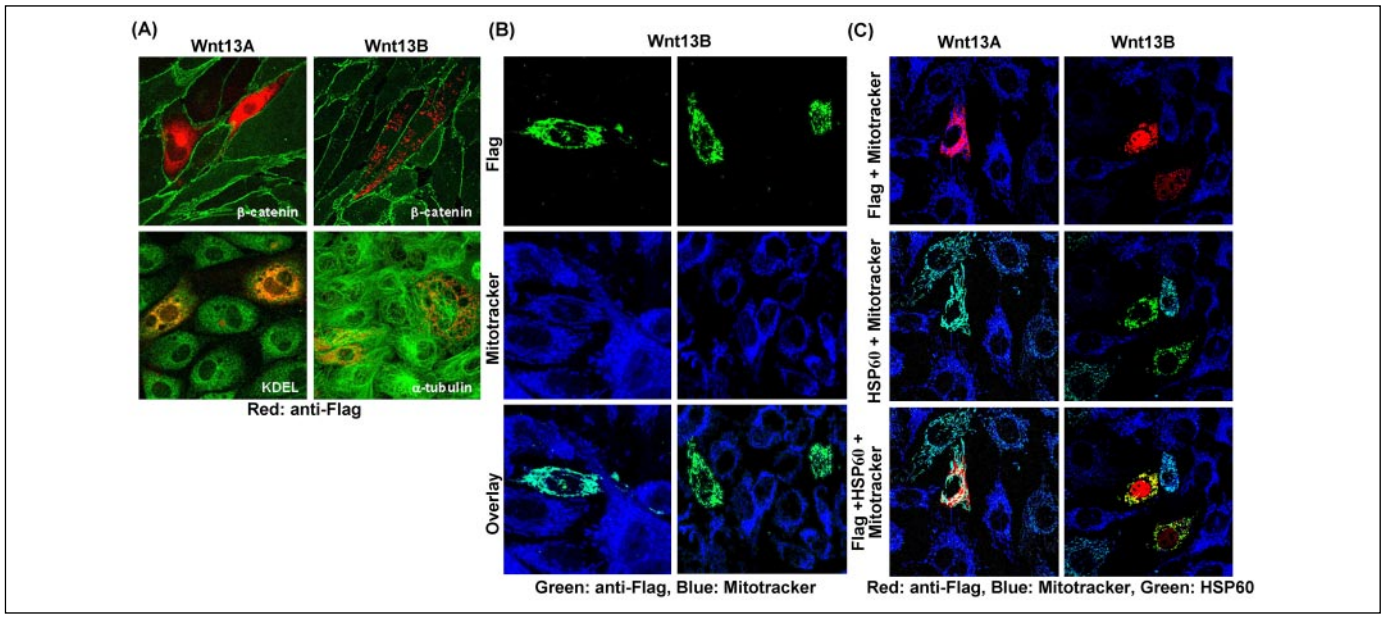

FIGURE 3. **Wnt13B co-localizes with mitochondrial markers.** *A*, Wnt13A and Wnt13B proteins display differential subcellular localizations. BAEC were transfected with Wnt13A-FLAG or Wnt13B-FLAG constructs, and 24 h later, the cells were fixed with 4% formaldehyde, permeabilized in 0.1% Triton, and stained with anti-FLAG antibodies (*red*) and with either anti-β-catenin, anti-KDEL, or anti-α-tubulin antibodies (*green*) for co-localization purposes. *B* and *C*, Wnt13B proteins co-localize with mitochondrial markers. BAEC were transfected as indicated for 24 h prior to mitochondria staining with the mitochondrial marker Mitotracker-Deep Red-633 for 45 min (*blue*). After cell fixation and permeabilization, Wnt13B-FLAG proteins were stained with the rabbit polyclonal anti-FLAG antibodies (B, *green*; *C*, *red*), and the mitochondrial chaperonin HSP60 was stained with the mouse monoclonal anti-HSP60 (*C*, *green*) and appropriate Alexa-conjugated secondary antibodies. Representative images obtained by confocal microscopy are presented.

Wnt13B N Terminus Contains Mitochondrial Targeting Sequences—Various targeting sequences for import into mitochondria have been identified, and these targeting signals, including those targeting to the inner membrane, are cleavable N-terminal presequences positively charged that can adopt an amphiphatic α-helix structure (32). Since Wnt13A and Wnt13B proteins differ only by their N-terminal sequences and Wnt13B appears as a protein doublet, the possibility that the Wnt13B N terminus contains cleavable mitochondrial targeting sequences was first assessed. In addition to a very hydrophobic N terminus (aa 1–17), two putative amphiphatic α-helices containing positively charged residues are present; however, only the first one will be specific for Wnt13B (Fig. 4*A*). In contrast, the equivalent Wnt13A first α-helix is devoid of positively charged residues. To delineate their role in Wnt13 processing and localizations, the divergent N-terminal α-helices of Wnt13A and Wnt13B were swapped to generate the chimeric proteins Wnt13AB (Wnt13-A(1–42)B(26–372)-FLAG) and Wnt13BA (Wnt13-B(1–25)A(43–391)) (Fig. 4*A*). As shown in Fig. 4*B*, the chimeric Wnt13BA-FLAG proteins, containing the N-terminal hydrophobic stretch of Wnt13B fused to the putative α-helix of Wnt13A signal peptide, appear as a single protein band of 42 kDa in size like Wnt13A proteins. In addition, Wnt13BA-FLAG proteins are also *N*-glycosylated like Wnt13A proteins as demonstrated by their sensitivity to tunicamycin treatment. In contrast, the chimeric Wnt13AB-FLAG proteins containing the first putative amphiphatic α-helix of Wnt13B but lacking the N-terminal hydrophobic stretch of Wnt13B are un-*N*-glycosylated like Wnt13B-FLAG proteins. However, Wnt13AB-FLAG proteins appear as a single protein band of 41 kDa in size not as a protein doublet like Wnt13B-FLAG proteins (Fig. 4*B*). The slight difference in size between Wnt13AB-FLAG proteins and L-Wnt13B-FLAG proteins corresponds to the additional 17 residues in length of the N terminus of Wnt13AB compared with Wnt13B (Fig. 4*A*). Nonetheless, the chimeric Wnt13AB proteins were localized to mitochondria like Wnt13B proteins, although there was an increase of the nuclear localization (Fig. 5). The chimeric Wnt13BA proteins localized mainly in the ER like Wnt13A proteins, in agreement with their similar processing (Fig. 5). These results are thus compatible with a role of the first α-helix of Wnt13A in its targeting to the ER and of the first α-helix of Wnt13B in its targeting to mitochondria.

The analysis of Wnt13B N-terminal sequences using MitoProt II program (33) gave a putative cleavage site for mitochondrial import between Val^{51} and Ile^{52} with positively charged residues in position −2 (Arg^{50}) and −10 (Arg^{42}) from the cleavage site, whereas similar analysis using the PSORT program (available on the World Wide Web at www.PSORT.nibb.ac.jp) gave a cleavage site between Tyr^{70} and Pro^{71}, based on the presence of Arg^{69} at position −2 (34) (Fig. 4*A*). From these predictions, three N terminus deletion mutants of Wnt13B were generated: Δ(1–17)Wnt13B, which is lacking the N-terminal hydrophobic stretch, Δ(1–52)Wnt13B-FLAG, which is further lacking the first α-helix and the putative $RV^{51} \downarrow I^{52}$ cleavage site, and Δ(1–88)Wnt13B-FLAG, which is further lacking the putative $RY^{70} \downarrow P^{71}$ cleavage site and part of the second amphiphatic α-helix. As shown in Fig. 4*C*, the Δ(1–17)Wnt13B-FLAG and Δ(1–52)Wnt13B-FLAG mutants appeared mainly as single protein bands of 39- and 37-kDa apparent size, respectively, that are in agreement with the deletions made in L-Wnt13B. The S-Wnt13B form was still observed with both deletion mutants, but the levels were far less abundant than in wild type Wnt13B (Fig. 4*C*). With the Δ(1–88)Wnt13B-FLAG mutants, the appearance of a protein doublet was completely abolished, since a single protein band of 34 kDa, lower than the S-Wnt13B form, was observed (Fig. 4*C*). Δ(1–17)Wnt13B-FLAG proteins, like wild type Wnt13B proteins, were mainly localized in mitochondria, although a slight increase in the nuclear localization was observed as with the chimera Wnt13AB (not shown). In contrast, Δ(1–52)Wnt13B-FLAG proteins displayed only a residual co-localization with both mitochondrial markers, HSP60 and Mitotracker, and most of the mutant proteins were found in the nuclei (Fig. 5). The ability of Mitotracker to accumulate in mitochondria was less affected in cells expressing Δ(1–52)Wnt13B-FLAG proteins than in cells expressing wild type Wnt13B-FLAG proteins, although mitochon-

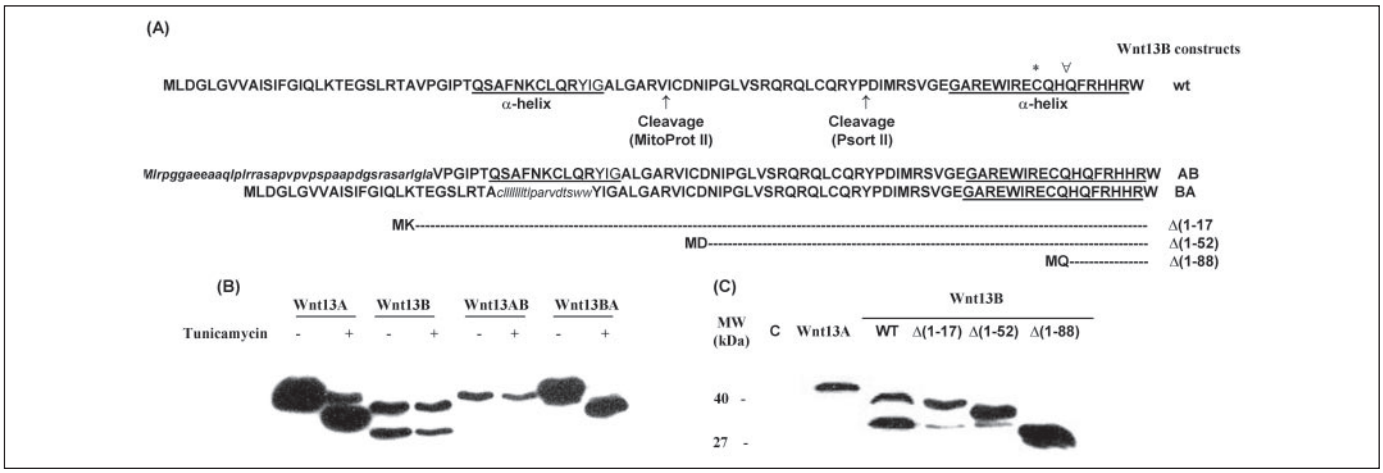

FIGURE 4. **Wnt13B N-terminal sequences contain mitochondrial targeting sequences.** *A*, the unique N-terminal sequence of Wnt13B is in *boldface type*, and the two putative amphiphatic α-helices are *underlined*. Two putative cleavage sites predicted either by MitoProt II or by PSORT are indicated with *arrows*. The conserved Cys^{88} palmitoylation site (*) and Gln^{91} *N*-glycosylation site (∀) are also indicated. The N-terminal Wnt13A/Wnt13B chimeras and the N terminus deletion mutants of Wnt13B generated in this study are represented. Wnt13A-specific sequences in Wnt13AB and Wnt13BA chimeras are in *italic type*. *B*, analysis of the processing of the chimeras of Wnt13A and Wnt13B N termini. BAEC were transiently transfected with the various constructs as indicated and were either left untreated (−) or treated with 5 μg/ml tunicamycin for 20 h. *C*, Western blot analysis of wild type and N-terminal deletion mutants of Wnt13B. BAEC were transiently transfected either with control (*C*) or with the various Wnt13B deletion constructs as indicated. In all cases (*B* and *C*), whole cell extracts were prepared 24 h after transfection and analyzed on 10% polyacrylamide-SDS gel followed by immunoblotting for detection of the FLAG-tagged proteins.

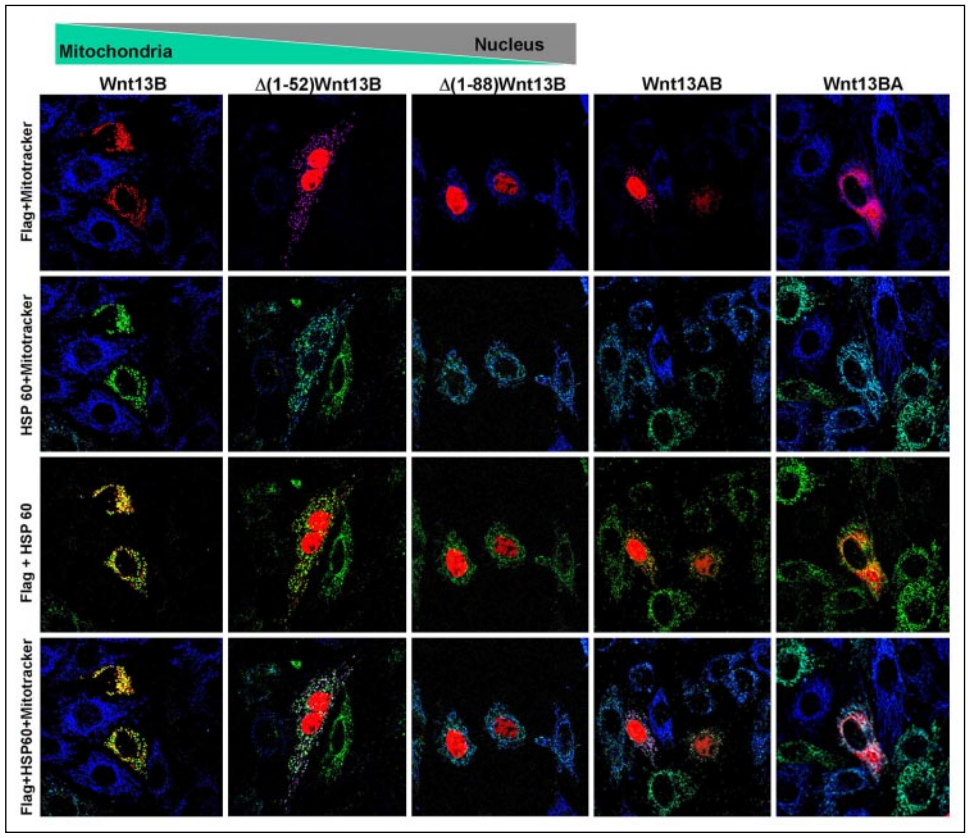

FIGURE 5. **Localization of Wnt13B in mitochondria is dependent upon its N-terminal sequences.** The co-localization of wild type, N-terminal chimeras, and N-terminal deletion mutants of Wnt13B-FLAG proteins (*red*) with Mitotracker-Deep Red-633 (*blue*) and the mitochondrial chaperone HSP60 (*green*) was assessed by confocal immunofluorescence microscopy in transiently transfected BAEC as described under "Materials and Methods." Representative images are shown.

dria fragmentation was also observed. The mitochondrial targeting was completely lost in the Δ(1–88)Wnt13B mutants, since they were only localized within nuclei (Fig. 5). These results are also compatible with mitochondrial targeting sequences located in the N terminus of Wnt13B and pinpoint both the N-terminal hydrophobic stretch and the first α-helix as main determinants.

Dissociation between the Mitochondrial Targeting and the Production of S-Wnt13B—Since the S-Wnt13B form displayed an intermediate size between Δ(1–52)Wnt13B-FLAG and Δ(1–88)Wnt13B-FLAG, these results suggested that if S-Wnt13B results from a proteolytic cleavage during the targeting to mitochondria, the cleavage site was close to the putative $Tyr^{70} \downarrow Pro^{71}$ site instead of the $Val^{51} \downarrow Ile^{52}$ site. However, attempts to determine whether the S-Wnt13B form arises from proteolytic cleavage of the L-Wnt13B form using various inhibitors of degradation pathways (*i.e.* inhibitors of the proteasome, calpain, lysosome, and caspase activities) as well as inhibitors of metalloprotease activities to inactivate the mitochondrial processing peptidase gave inconsistent results (not shown). Therefore, targeted mutations were designed to pinpoint the mechanism of generation

TABLE 2
Summary of the characterization and localization of Wnt13 isoforms and mutants

Name	*N*-Glycosylation	Doublet	Localization
Wnt13A	+	−	ER
Wnt13B	−	+	Mitochondria > nucleus
Wnt13C	−	−	Nucleus
Wnt13AB	−	−	Mitochondria > nucleus
Wnt13BA	+	−	ER
Δ(1–17)Wnt13B	ND[a]	+/−	Mitochondria > nucleus
Δ(1–52)Wnt13B	ND	−	Nucleus ⋙ mitochondria
Δ(1–88)Wnt13B	ND	−	Nucleus
R50A-Wnt13B	ND	+	Mitochondria > nucleus
R69G-Wnt13B	ND	+	Mitochondria > nucleus
K38A,R42A,R50A-Wnt13B	ND	+	Mitochondria-nucleus
R62A,R64A,R69G-Wnt13B	ND	+	Mitochondria > nucleus
M74L-Wnt13B	ND	−	Mitochondria
D72E-Wnt13B	ND	+	Mitochondria > nucleus
R75A-Wnt13B	ND	+	Mitochondria > nucleus
M1L-Wnt13B	ND	−	Nucleus

[a] ND, not determined.

of the S-Wnt13B form and its association with Wnt13B mitochondrial targeting, and the results are summarized in Table 2. The targeted mutations eliminating the Arg residue in position −2 of the putative mitochondrial cleavage sites, R69G-Wnt13B and R50A-Wnt13B, affected neither the appearance of the S-Wnt13B form nor the localization of the mutant proteins in mitochondria. Similarly, mutations of each positively charged amino acid either in the first α-helix of Wnt13B ((K38A,R42A,R50A)-Wnt13B) or upstream of the putative $Tyr^{70} \downarrow Pro^{71}$ cleavage site ((R62A,R64A,R69G)-Wnt13B) did not affect the appearance of the Wnt13B protein doublet. A mitochondrial localization was still observed for both triple mutants, although the (K38A,R42A,R50A)-Wnt13B mutant displayed more nuclear localization than wild type Wnt13B (Table 2).

Thus, the positively charged residues located either in the first α-helix (38–50) or in positions 62–69 of the Wnt13B N-terminal sequence are dispensable for the mitochondrial targeting, and there are no mitochondrial proteolytic cleavages taking place in either the $Val^{51} \downarrow Ile^{52}$ or $Tyr^{70} \downarrow Pro^{71}$ positions. The latter results in conjunction with our results with the chimera Wnt13AB and the deletion Δ(1–17)Wnt13B mutants suggest that the generation of the S-Wnt13B form is separate from the mitochondrial targeting.

S-Wnt13B Is Generated via the Alternative Met^{74} Translation Start Site—Among the various aa changes generated in Wnt13B N-terminal sequences to delineate their role in Wnt13B processing and localization, the Wnt13B protein doublet was completely abolished only with the M74L-Wnt13B mutant (Table 2). In contrast, targeted mutations surrounding Met^{74}, such as D72E and R75A, had no effect on the Wnt13B protein doublet, since both L-Wnt13B and S-Wnt13B forms were observed (Table 2). With the M74L-Wnt13B mutant, only the long form of Wnt13B was observed (Fig. 6*B*), indicating that the use of an alternative translation start site, Met^{74}, might be responsible for the generation of S-Wnt13B. To further test this hypothesis, the reciprocal mutation of the first translation start site was generated. As shown in Fig. 6*B*, the Wnt13B protein doublet was also abolished with the M1L-Wnt13B mutant, since only the S-Wnt13B form was observed. To rule out any possible spurious RNA splicing occurring in Wnt13B-transfected cells that eliminates the first ATG, the expression of the various Wnt13 mRNA species in BAEC transfected with the human Wnt13B cDNA was controlled by reverse transcription-PCR. Human-Wnt13B cDNA was the only Wnt13 cDNA that could be amplified with the specific human primers located in exons 1 and 4 (Fig. 6*C*). Smaller human Wnt13 cDNAs, even the human Wnt13C splice variant identified in this study, were undetectable in Wnt13B-transfected BAEC (Fig. 6*C*). Altogether these results demonstrated that the L-Wnt13B form is encoded from the first ATG encountered in Wnt13B mRNA, whereas the S-Wnt13B form is generated from the same mRNA species via the use of an alternative translation start site located 73 codons downstream of the first ATG and codes for Met^{74} in L-Wnt13B. The subcellular localization of M1L-Wnt13B and M74L-Wnt13B, equivalent to S-Wnt13B and L-Wnt13B, respectively, were determined by confocal immunofluorescence microscopy. In transfected BAEC, M1L-Wnt13B/S-Wnt13B localized mainly to the nucleus, whereas only a residual association with mitochondria was observed (Fig. 6*D*) and thus behaved similarly to Δ(1–52)Wnt13B (Fig. 5). In contrast, M74L-Wnt13B/L-Wnt13B were mainly localized to mitochondria (Fig. 6*D*), and the small nuclear localization observed with Wnt13B (Fig. 3) was greatly reduced, since less than 3% of the M74L-Wnt13B-expressing cells display a nuclear staining. Thus, when S-Wnt13B and L-Wnt13B are expressed alone, their subcellular localizations can be distinguished, since they are targeted mainly to the nucleus and mitochondria, respectively. These subcellular localizations were also confirmed by cell fractionation (Fig. 6*E*). Indeed, M74L-Wnt13B/L-Wnt13B co-fractionate with the mitochondrial protein apoptosis-inducing factor, whereas M1L-Wnt13B is mainly associated with the nuclear fraction (Fig. 6*E*). Wnt13B was present mainly in the mitochondria enriched fraction and to a lesser extent in the nuclear fraction, similar to how it was observed by immunofluorescence microscopy. Wnt13A co-fractionated mainly with the ER marker calnexin but was also found associated with light membrane fractions. All of the transfected Wnt13 forms were present also in the ER fraction, since this fraction includes also the rough ER, where their synthesis is taking place. As was previously noticed with Wnt13A (Fig. 2*A*), stable homodimers of M1L-Wnt13B or of M74L-Wnt13B were also observed in transfected BAEC (Fig. 6*F*). In Wnt13B-transfected BAEC, three dimer bands were observed corresponding to S-Wnt13B homodimers and L-Wnt13B homodimers as they co-migrated with M1L-Wnt13B and M74L-Wnt13B homodimers, respectively, as well as an intermediary band corresponding to S-Wnt13B/L-Wnt13B heterodimers (Fig. 6*F*).

S-Wnt13B Is Equivalent to Wnt13C—In light of these results, the deduced N-terminal sequence for Wnt13C (Figs. 1 and 6*A*) had to be revisited, since Wnt13C mRNAs could also be translated from the second ATG and encode a protein equivalent to S-Wnt13B. To test this hypothesis, the FLAG tag coding sequence was inserted in Wnt13C cDNA in the same place and frame as in Wnt13B cDNA (see "Materials and Methods" and Table 1). In BAEC transfected with Wnt13C-FLAG constructs, Wnt13C proteins appeared as a single protein band similar in size to S-Wnt13B and M1L-Wnt13B (Fig. 6*B*) and also localized in the nucleus (Fig. 6*E*). Therefore, our results demonstrate that S-Wnt13B and Wnt13C proteins are undistinguishable and that Wnt13C nuclear forms are translated from both Wnt13B and Wnt13C mRNAs.

Nuclear Forms of Wnt13 Increase β-Catenin-TCF Activity in HEK293 Cells—Since the β-catenin/TCF pathway is not functional in BAEC (not shown), the effects of the various Wnt13 forms on the activation of this pathway were determined in HEK293 cells using the standard TOP-Flash luciferase reporter assay (30). None of Wnt13 forms, including Wnt13A, induced directly an activation of the β-catenin/TCF activity in HEK293 as measured by the TOP-Flash luciferase reporter assay (not

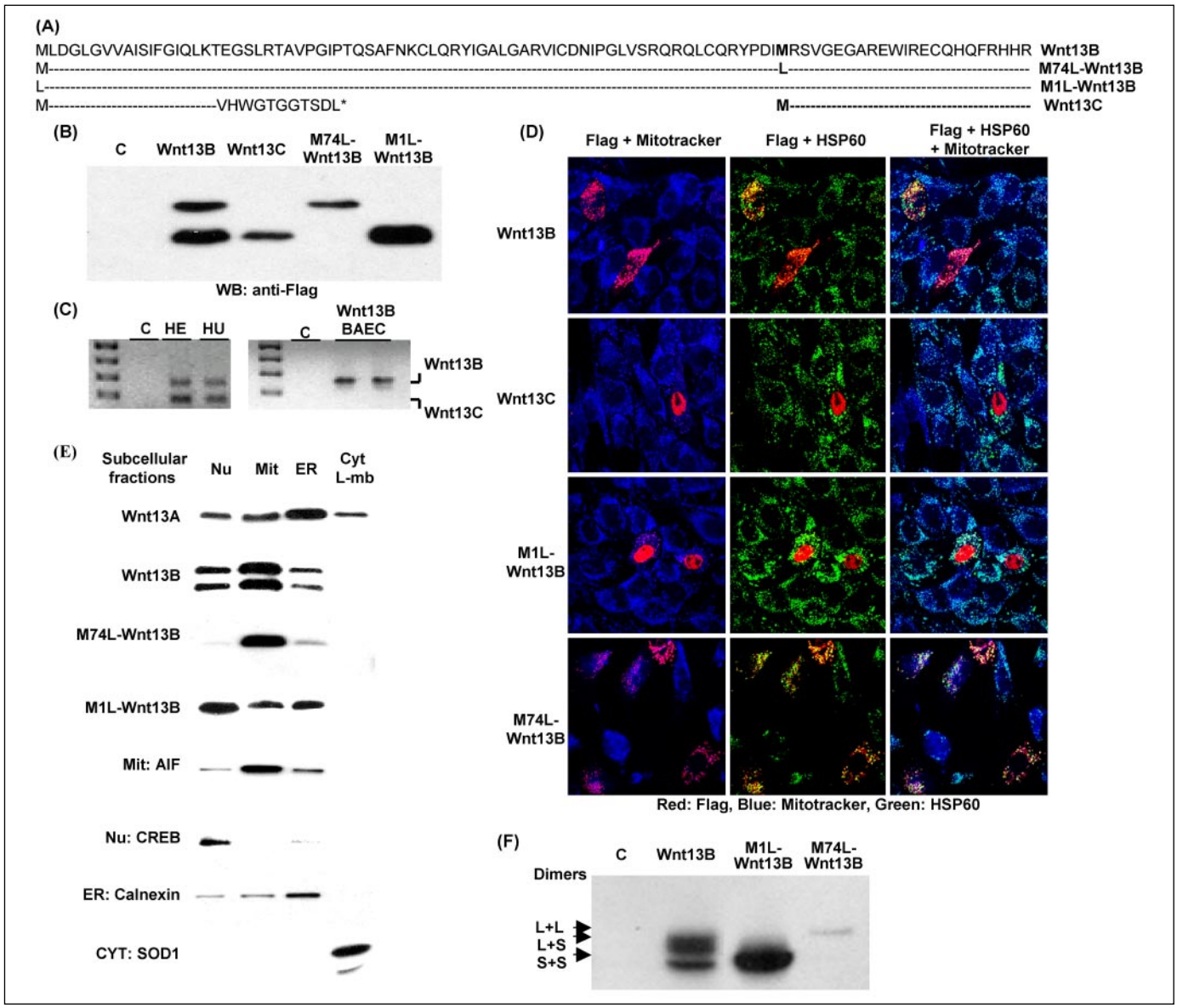

FIGURE 6. **The S-Wnt13B form is generated via the use of an alternative translation start, Met^{74}.** *A*, representation of the N-terminal sequences of Wnt13B, Wnt13C, and of the M1L- and M74L-Wnt13B mutants. *B*, analysis of the expression of Wnt13C-FLAG proteins and of M1L- and M74L-Wnt13B-FLAG mutants in BAEC. BAEC were transiently transfected with the indicated constructs, and 24 h later, whole cell extracts were prepared, and the FLAG-tagged proteins were detected by immunoblotting. *C*, analysis of the Wnt13 mRNA species expressed in Wnt13B-transfected BAEC by reverse transcription-PCR. BAEC were transfected with the huWnt13B construct for 18 h prior to total RNA isolation, removal of DNA contaminations, and reverse transcription as described under "Materials and Methods." Wnt13 cDNAs were amplified using the forward Wnt13B/C primer located in exon 1 and the reverse Wnt13 universal primer located in exon 4 and were resolved on 2% agarose gels. As a control, the endogenous Wnt13B and -C mRNA isoforms were similarly amplified using total RNA from HEK293 cells and HUVEC. *D*, analysis of the subcellular localization of Wnt13C-FLAG and of M1L-Wnt13B and M74L-Wnt13B-FLAG mutants by confocal immunofluorescence microscopy as previously described. Representative images are shown. *E*, analysis of the subcellular localization of the various Wnt13 forms by cell fractionation and immunoblotting. The quality of the different subcellular fractions was monitored using calnexin as an ER marker, AIF as a mitochondrial marker, CREB as a nuclear marker, and SOD1 as a cytosolic marker. *F*, analysis of Wnt13B dimers. BAEC were transiently transfected with the indicated constructs, and 24 h later, whole cell extracts were prepared, and the FLAG-tagged proteins were separated on nondenaturing 8% polyacrylamide gels and detected by immunoblotting.

shown). However, the nuclear forms induced a significant 2.3-fold increase of the β-catenin/TCF activity in HEK293 cells co-transfected with the stable mutant S37A-β-catenin, whereas M74L-Wnt13B, Wnt13B and Wnt13A had no effect (Fig. 7*A*). This increase of β-catenin/TCF activity was not due to an increase of the expression or stability of S37A-β-catenin, since similar amounts of HA-S37A-β-catenin were observed across the various co-transfections (Fig. 7*A*). We next tested, using real time PCR, whether the nuclear forms of Wnt13 were also able to increase the expression of IL-8, a known β-catenin target gene (35). As shown in Fig. 7*B*, the expression of IL-8 mRNA in HEK293 cells was increased by the nuclear form M1L-Wnt13B alone and in combination with S37A-β-catenin about 2- and 3-fold, respectively, as compared with the control. The 2.2-fold further increase of IL-8 mRNA expression obtained with the combination M1L-Wnt13B/S37A-β-catenin as compared with S37A-β-catenin alone is in agreement with the increase of β-catenin/TCF activity observed with the same combination in Fig. 7*A*.

Nuclear Forms of Wnt13 Increase Apoptosis in BAEC—The main characteristic of Wnt13B-expressing cells was the fragmented morphology of the mitochondrion as well as a decreased ability to accumulate the Mitotracker dye (Figs. 3 and 5). Since mitochondria fragmentation is an early event in the cascade leading to apoptotic cell death (36), the possibility that Wnt13B was inducing apoptosis in BAEC was tested. For this purpose, the percentage of apoptotic nuclei in Wnt13B-expressing cells was determined (Fig. 8*A*). As compared with cells express-

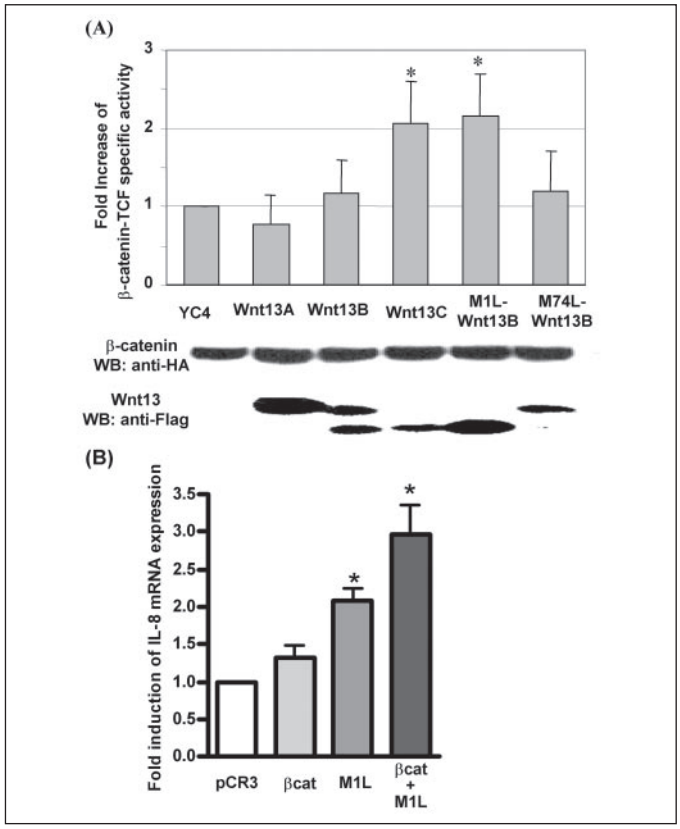

FIGURE 7. **Wnt13 nuclear forms increase β-catenin-TCF activity in HEK293 cells.** *A*, analysis of the transcriptional β-catenin/TCF activity by luciferase assays. HEK293 cells were co-transfected with a normalization control vector (phRG-TK), the degradation-resistant β-catenin mutant (S37A-β-catenin), the TCF/LEF reporter construct TOP-Flash, or the mutated FOP-Flash construct and the various Wnt13 constructs or YC4-mit construct as control. Luciferase activities were quantified by dual luciferase assays, and, after normalization of the firefly luciferase activity *versus Renilla* luciferase activity, the ratio of the specific β-catenin/TCF activity (TOP-Flash) *versus* unspecific activity (FOP-Flash) was determined. The results are expressed as -fold increase of the ratio TOP-Flash/FOP-Flash in Wnt13-transfected cells *versus* control-transfected cells (YC4-mit). S.D. values are indicated; *, differences were significant at $p < 0.01$ (*t* test, analysis of variance). *B*, analysis of the induction of IL-8 mRNA expression by real time PCR. HEK293 cells were transfected either with pCR3 (*pCR3*), pcDNA3-S37A-β-catenin (*βcat*), pCR3-M1L-Wnt13B (*M1L*), or the combination pcDNA3-S37A-β-catenin + pCR3-M1L-Wnt13B (*βcat+M1L*) for 24 h prior to total RNA extraction. The levels of IL-8 mRNA expression were monitored by real time PCR and normalized with the expression of rpL32 mRNA as indicated under "Materials and Methods." The -fold induction of IL-8 mRNA expression was determined against the control (pCR3 = 1). Mean and S.E. values of the -fold induction of IL-8 expression obtained in four independent transfection experiments are reported in the graph; *, differences were significant at $p < 0.01$ (*t* test, analysis of variance).

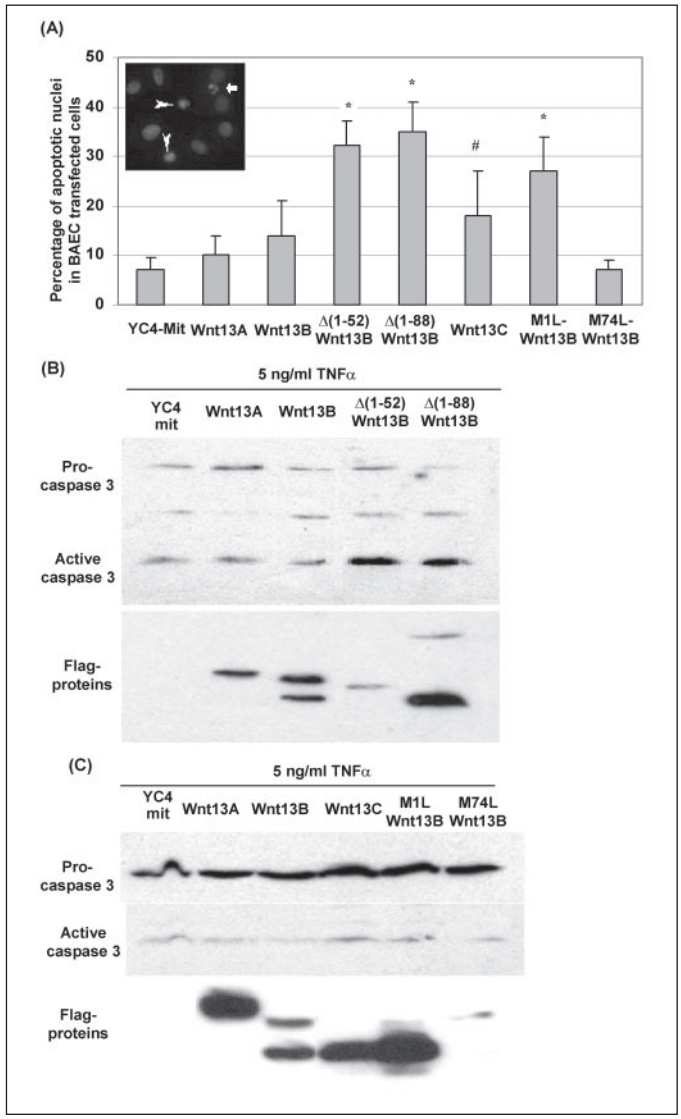

FIGURE 8. **Wnt13 nuclear forms increased apoptosis in BAEC.** *A*, quantification of apoptotic nuclei in BAEC expressing cells. BAEC were transfected with the various constructs as indicated, and 36 h later the cells were fixed, permeabilized, and stained with the anti-FLAG antibodies. The nuclei were stained with 4′,6-diamidino-2-phenylindole during slide mounting. Images of 100 cells expressing either FLAG epitope (Wnt13) or green fluorescent protein (YC4-mit) were taken in random fields for each of the constructs, and the numbers of fragmented (*arrows*) and condensed (*arrowheads*) nuclei as shown in the *inset* were determined. The results are expressed as a percentage of the total nuclei analyzed and are means of 3–5 independent experiments. S.D. values are indicated; differences were significant at $p < 0.01$ (*) and $p < 0.05$ (#) (*t* test, analysis of variance). *B* and *C*, analysis of caspase-3 activation. BAEC were transfected with the various constructs as indicated, and 20 h later, the cells were treated with 5 ng/ml of TNF-α for an additional 12-h period. Adherent and detached cells were combined, washed in PBS, and lysed. An equivalent amount of proteins was loaded on SDS-12% PAGE, and the presence of active cleaved caspase-3 fragment, procaspase-3, and FLAG-tagged proteins was analyzed by immunoblotting. Images from representative experiments are shown.

ing Wnt13A proteins or green fluorescent proteins targeted to the mitochondria matrix (YC4-mit), there was a slight increase in the percentage of apoptotic nuclei in cells expressing Wnt13B proteins (10% *versus* 7%), although it was not statistically significant. In contrast, signs of apoptotic nuclei were observed in 35% of the cells expressing the deletion mutant Δ(1–52)Wnt13B-FLAG and Δ(1–88)Wnt13B-FLAG proteins (Fig. 8*A*). Since these deletion mutants localize in the nuclei (Fig. 5), these results suggest that the increase in cell apoptosis is associated with the nuclear localization of Wnt13B proteins rather than with its mitochondrial localization. In agreement with this hypothesis, the expression of the nuclear Wnt13C and M1L-Wnt13B proteins was also associated with an increase of the appearance of apoptotic nuclei in BAEC, 18 and 27% in expressing cells, respectively, whereas the expression of M74L-Wnt13B proteins had similar effects as the control proteins (5% *versus* 7%) (Fig. 8*A*). The activation of caspase-3, another marker of apoptosis was undetectable in BAEC transfected with the various constructs in the absence of further apoptotic stimuli (not shown). However, in the presence of a low dose of TNFα (5 ng/ml) for 12 h, the appearance of the active cleaved caspase-3 fragment can be followed by immunoblotting (Fig. 8, *B* and *C*). Under these conditions, an increase of the levels of active caspase-3 was observed in BAEC expressing the nuclear forms of Wnt13B, Δ(1–52)Wnt13B and Δ(1–88)Wnt13B (Fig. 8*B*), as well as Wnt13C and M1L-Wnt13B (Fig. 8*C*), compared with BAEC expressing the mitochondrial targeted green fluorescent protein (YC4-mit), Wnt13A, Wnt13B, or the mitochondrial M74L-Wnt13B (Fig. 8, *B* and *C*).

DISCUSSION

Altogether the results presented in this report reveal the complexity of *wnt13* expression, since combinations of alternative promoters, alternative RNA splicing, and alternative translation start sites are used to generate three Wnt13 protein isoforms displaying different intracellular localizations. Alternative promoters and alternative RNA splicing give rise to three different mRNA species, the previously described Wnt13A/Wnt2B2 and Wnt13B/Wnt2B1 mRNAs (20) and a novel Wnt13C mRNA (Fig. 1), which are expressed in all the endothelial cell lines tested (Fig. 1). In addition, Wnt13B mRNA was shown to encode two proteins via the use of alternative translation start sites, L-Wnt13B and S-Wnt13B forms. The latter is identical to the Wnt13C protein encoded by Wnt13C mRNA, since the same translation start site is used (Fig. 6). Although this is the first report demonstrating the presence of alternative translation start sites in Wnt mRNAs, this is a mechanism known to regulate the spatio-temporal expression of various proteins involved in development as well as to increase the diversity of their N-terminal sequences, which results in different subcellular localizations and activities (37). For example, nuclear and cytoplasmic forms of fibroblast growth factor-2 displaying different transforming activities are produced through such alternative translation initiation sites (38).

We have demonstrated for the first time that two isoforms of Wnt13 proteins, L-Wnt13B and S-Wnt13B/Wnt13C, are targeted to mitochondria and to the nucleus rather than to the ER and the secretory pathway like Wnt13A (Figs. 3 and 6) and most of the Wnt proteins (11–13). Previously, Wnt13A/Wnt2B2 was shown to induce the duplication axis in *Xenopus* embryos and to activate the β-catenin pathway, whereas Wnt13B/Wnt2B1 failed to do so (25). Our results, demonstrating the different subcellular localization for Wnt13A and both forms of Wnt13B (Figs. 3 and 6), explain the differential activities observed. L-Wnt13B and Wnt13A differ only by their N-terminal sequences, and herein we have shown that the α-helix of L-Wnt13B, located between residues 26 and 50, and the α-helix of Wnt13A containing the leucine stretch of the signal peptide are key determinants for targeting to mitochondria and to the ER, respectively (Figs. 4 and 5). All forms lacking these N-terminal sequences, such as Wnt13C/S-Wnt13B and the Δ(1–52)Wnt13 and Δ(1–88)Wnt13 deletion mutants, display predominantly a nuclear localization (Figs. 5 and 6). The N-terminal sequences are the most divergent domains among the Wnt family members, and they have previously been implicated in the different secretion efficiencies of the Wnt proteins (11). The N-terminal sequences of Wnt1 (residues 1–99) were shown to contain the main determinant distinguishing Wnt1 and Wnt5A in their ability to transform C57MG epithelial cells and to induce β-catenin stabilization (39). Our results reinforce the importance of these variable N-terminal sequences both in the processing and intracellular localization of the Wnt proteins and thus suggest additional diversity in their activities and mechanisms of action.

Localization of Wnt13B-FLAG proteins in mitochondria was demonstrated by co-localization with various markers of mitochondria: the Mitotracker dye that specifically accumulates in active mitochondria (40) and the mitochondrial matrix chaperone HSP60 (41). Wnt13B mitochondrial localization was confirmed by biochemical analysis of mitochondria enriched fractions, where both L-Wnt13B and S-Wnt13B forms could be detected (Figs. 2 and 6). In addition to this mitochondrial localization, we have observed that 10–20% of the cells expressing Wnt13B-FLAG proteins displayed also a nuclear localization (Fig. 3). These variable levels of nuclear localization can be accounted for by variable expression of S-Wnt13B, since this form is mainly nuclear (Fig. 6, *D* and *E*). Although the subcellular localization of L-Wnt13B in mitochondria and S-Wnt13B in nucleus can be detected unambiguously when they are expressed alone (Fig. 6, *D* and *E*), this was not possible when L-Wnt13B and S-Wnt13B are co-expressed together in Wnt13B cDNA-transfected cells. We have observed that L-Wnt13B/S-Wnt13B heterodimers are present in whole cell extracts as well as in mitochondrial fractions (Fig. 6, *B* and *E*), which can explain these discrepancies of localization. Similarly, the residual association with mitochondria of the nuclear forms, the Δ(1–52)Wnt13B deletion mutant and M1L-Wnt13B/S-Wnt13B mutant, might be due to the formation of heterodimers between the endogenous Wnt13B forms and the transfected mutated forms. Alternatively, residual interactions of Wnt13 nuclear forms with proteins involved in mitochondrial targeting, such as chaperones (41), might explain these observations. Wnt proteins have been previously shown to interact with chaperones located in the ER, such as Grp78-BiP, and this interaction was considered as the main cause of Wnt protein retention in the ER (13). In addition, such chaperone-mediated targeting of Wnt13 proteins could explain the intriguing absence of Wnt13 precursor proteins in the cytoplasm. Further work is needed to clearly delineate the role of Wnt13 dimerization and/or Wnt13 protein/protein interactions in its targeting.

Most of the proteins destined for the mitochondrial matrix as well as for the mitochondria inner membrane are initially synthesized as a precursor with cleavable N-terminal targeting presequences, which display amphiphatic α-helices able to interact with both the translocase outer membrane and the translocase inner membrane complexes (42). Although both the hydrophobic stretch (aa 1–17) and the α-helix (aa 26–50) of Wnt13B-specific N-terminal sequences were necessary for Wnt13B targeting to mitochondria (Fig. 5), they were insufficient to target a Wnt13B-(1–50)-green fluorescent protein fusion protein to mitochondria (not shown). Also, mutations of all of the positively charged residues in Wnt13B α-helix or surrounding putative mitochondrial cleavage sites, (K38A,R42A,R50A)-Wnt13B and (R62A,R64A,R69G)-Wnt13B mutants, did not affect the mitochondrial targeting (Table 2). Altogether these results indicate that Wnt13B targeting to mitochondria appears independent of the interaction with the translocase outer membrane/translocase inner membrane complexes and suggest that additional domains, such as a chaperone interaction domain or the overall structure of Wnt13 proteins, are also necessary for the mitochondrial targeting. Similarly, the nuclear Wnt13C proteins are lacking typical nuclear localization sequences. Although their small size (<40 kDa) should enable a free diffusion across the nuclear pore, Wnt13C nuclear translocation might be chaperone-mediated.

Wnt13B proteins were tightly associated with mitochondrial membranes, even in mitoplasts lacking the outer membrane (Fig. 2*C*). Mutation of Wnt13B-cysteine 88, which corresponds to the conserved cysteine being modified by palmitoylation in several Wnt proteins during their transit in the ER (18, 19), had no effect on Wnt13B mitochondrial targeting (Table 2). This lack of effect is consistent with a palmitoylation modification of the Wnt proteins taking place specifically in the ER like the *N*-glycosylation modifications. Further work is needed to determine whether other lipid modifications of L-Wnt13B are responsible for the targeting to mitochondria or whether L-Wnt13B is an inherent membrane protein.

In Wnt13B-expressing cells, mitochondria displayed a fragmented morphology and a reduced ability to accumulate Mitotracker dye (Figs. 3 and 5). Mitochondria fragmentation occurs physiologically during cell replication and division but also during apoptosis (36). Wnt13B localization to mitochondria was not clearly associated with apoptosis, whereas expression of Wnt13 nuclear forms increased significantly the number of apoptotic nuclei (Fig. 8*A*) and rendered BAEC more suscep-

tible to TNF-α-induced apoptosis (Fig. 8, *B* and *C*). The effects of the nuclear forms on apoptosis might be associated with their effects on β-catenin/TCF activities, since this pathway has also been involved in apoptosis (43). In agreement with the lack of apoptosis, the ATP production was not significantly altered in Wnt13B-transfected cells (not shown); therefore, the reduced accumulation of the Mitotracker dye could not be explained by inactive mitochondria. Since Wnt13B in mitochondria is associated with the membranes, it is conceivable that the diffusion of Mitotracker to the mitochondrial membranes is prevented when Wnt13B proteins are in excess. On the other hand, Wnt proteins and Wnt signaling components have been implicated in cell division and differentiation (44, 45). Cell division requires coordinated nuclear and mitochondrial divisions as well as redistribution of organelles, including mitochondria, to the daughter cells (46). Therefore, the possibility that Wnt13B and Wnt13C play a role in the constant cross-talk between mitochondria and nucleus is worth testing.

Acknowledgments—We thank Dr. Paul E. DiCorleto for kindly providing the primary BAEC and HUVEC used in this study, Drs. Nicolas Demaurex and Stephen Byers for sharing the mitochondria-targeted YC4 and S37A-β-catenin-HA constructs, respectively, and Joel Thompson and Derek Adams for technical help.

REFERENCES

1. Wodarz, A., and Nusse, R. (1998) *Annu. Rev. Cell Dev. Biol.* **14,** 59–88
2. Strutt, D. (2003) *Development* **130,** 4501–4513
3. He, X., Semenov, M., Tamai, K., and Zeng, X. (2004) *Development* **131,** 1663–1677
4. Boutros, M., and Mlodzik, M. (1999) *Mech. Dev.* **83,** 27–37
5. Sheldahl, L. C., Slusarski, D. C., Pandur, P., Miller, J. R., Kuhl, M., and Moon, R. T. (2003) *J. Cell Biol.* **161,** 769–777
6. Peifer, M., and Polakis, P. (2000) *Science* **287,** 1606–1609
7. Veeman, M. T., Axelrod, J. D., and Moon, R. T. (2003) *Dev. Cell* **5,** 367–377
8. Mlodzik, M. (2002) *Trends Genet.* **18,** 564–571
9. Malliri, A., and Collard, J. G. (2003) *Curr. Opin. Cell Biol.* **15,** 583–589
10. Uusitalo, M., Heikkila, M., and Vainio, S. (1999) *Exp. Cell Res.* **253,** 336–348
11. Burrus, L. W., and McMahon, A. P. (1995) *Exp. Cell Res.* **220,** 363–373
12. Smolich, B. D., McMahon, J. A., McMahon, A. P., and Papkoff, J. (1993) *Mol. Biol. Cell* **4,** 1267–1275
13. Kitajewski, J., Mason, J. O., and Varmus, H. E. (1992) *Mol. Cell. Biol.* **12,** 784–790
14. Tanaka, K., Okabayashi, K., Asashima, M., Perrimon, N., and Kadowaki, T. (2000) *Eur. J. Biochem.* **267,** 4300–4311
15. van den Heuvel, M., Harryman-Samos, C., Klingensmith, J., Perrimon, N., and Nusse, R. (1993) *EMBO J.* **12,** 5293–5302
16. Kadowaki, T., Wilder, E., Klingensmith, J., Zachary, K., and Perrimon, N. (1996) *Genes Dev.* **10,** 3116–3128
17. Tanaka, K., Kitagawa, Y., and Kadowaki, T. (2002) *J. Biol. Chem.* **277,** 12816–12823
18. Willert, K., Brown, J. D., Danenberg, E., Duncan, A. W., Weissman, I. L., Reya, T., Yates, J. R. R., and Nusse, R. (2003) *Nature* **423,** 448–452
19. Zhai, L., Chaturvedi, D., and Cumberledge, S. (2004) *J. Biol. Chem.* **279,** 33220–33227
20. Katoh, M., Kirikoshi, H., Saitoh, T., Sagara, N., and Koike, J. (2000) *Biochem. Biophys. Res. Commun.* **275,** 209–216
21. Kubo, F., Takeichi, M., and Nakagawa, S. (2003) *Development* **130,** 587–598
22. Jasoni, C., Hendrickson, A., and Roelink, H. (1999) *Dev. Dyn.* **215,** 215–224
23. Liu, H., Mohamed, O., Dufort, D., and Wallace, V. A. (2003) *Dev. Dyn.* **227,** 323–334
24. Nakagawa, S., Takada, S., Takada, R., and Takeichi, M. (2003) *Dev. Biol.* **260,** 414–425
25. Katoh, M., Kirikoshi, H., Terasaki, H., and Shiokawa, K. (2001) *Biochem. Biophys. Res. Commun.* **289,** 1093–1098
26. Arnaudeau, S., Kelley, W. L., Walsh, J. V. J., and Demaurex, N. (2001) *J. Biol. Chem.* **276,** 29430–29439
27. DiCorleto, P. E., and de la Motte, C. A. (1985) *J. Clin. Invest.* **75,** 1153–1161
28. Cartron, P. F., Priault, M., Oliver, L., Meflah, K., Manon, S., and Vallette, F. M. (2003) *J. Biol. Chem.* **278,** 11633–11641
29. Lynn, B. D., Turley, E. A., and Nagy, J. I. (2001) *J. Neurosci. Res.* **65,** 6–16
30. Korinek, V., Barker, N., Morin, P. J., van Wichen, D., de Weger, R., Kinzler, K. W., Vogelstein, B., and Clevers, H. (1997) *Science* **275,** 1784–1787
31. Gavin, B. J., McMahon, J. A., and McMahon, A. P. (1990) *Genes Dev.* **4,** 2319–2332
32. Neupert, W. (1997) *Annu. Rev. Biochem.* **66,** 863–917
33. Claros, M. G., and Vincens, P. (1996) *Eur. J. Biochem.* **241,** 779–786
34. Gavel, Y., and von Heijne, G. (1990) *Protein Eng.* **4,** 33–37
35. Levy, L., Neuveu, C., Renard, C.-A., Charneau, P., Branchereau, S., Gauthier, F., Tran Van Nhieu, J., Cherqui, D., Petit-Bertron, A.-F., Mathieu, D., and Buendia, M. A. (2002) *J. Biol. Chem.* **277,** 42386–42393
36. Karbowski, M., and Youle, R. J. (2003) *Cell Death Differ.* **10,** 870–880
37. Pickering, B. M., and Willis, A. E. (2005) *Semin. Cell Dev. Biol.* **16,** 39–47
38. Bugler, B., Amalric, F., and Prats, F. (1991) *Mol. Cell. Biol.* **11,** 573–577
39. Julius, M. A., Rai, S. D., and Kitajewski, J. (1999) *Oncogene* **18,** 149–156
40. Poot, M., Zhang, Y. Z., Kramer, J. A., Wells, K. S., Jones, L. J., Hanzel, D. K., Lugade, A. G., Singer, V. L., and Haugland, R. P. (1996) *J. Histochem. Cytochem.* **44,** 1363–1372
41. Voos, W., and Rottgers, K. (2002) *Biochim. Biophys. Acta* **1592,** 51–62
42. Voos, W., Martin, H., Krimmer, T., and Pfanner, N. (1999) *Biochim. Biophys. Acta* **1422,** 235–254
43. Wong, M. H., Rubinfeld, B., and Gordon, J. I. (1998) *J. Cell Biol.* **4,** 765–777
44. Lu, B., Jan, L. Y., and Jan, Y. N. (1998) *Curr. Opin. Genet. Dev.* **8,** 392–399
45. Goldstein, B. (2000) *Dev. Dyn.* **218,** 23–29
46. Yaffe, M. P. (1999) *Science* **283,** 1493–1497
47. Daugas, E., Nochy, D., Ravagnan, L., Loeffler, M., Susin, S. A., Zamzami, N., and Kroemer, G. (2000) *FEBS Lett.* **476,** 118–123